Discover Nano

RESEARCH Open Access

Photocatalytic degradation of tetracycline by TiO_2/PVDF film photocatalyst: degradation mechanism and intermediates analysis

Hazlini Mohmad Ameran[1,2], Abdul Halim Abdullah[1*], Yen Ping Tan[1], Ernee Noryana Muhamad[1], Teruhisa Ohno[3*] and Yoshito Ando[4]

*Correspondence:
Abdul Halim Abdullah
halim@upm.edu.my
Teruhisa Ohno
tohno@che.kyutech.ac.jp
[1]Department of Chemistry, Faculty of Science, Universiti Putra Malaysia, 43400 Serdang, Selangor, Malaysia
[2]Department of Chemistry, Center of Foundation studies, UiTM Cawangan Selangor, Kampus of Dengkil, 43800 Sepang, Selangor, Malaysia
[3]Department of Applied Chemistry, Faculty of Engineering, Kyushu Institute of Technology, Fukuoka 804-8550, Japan
[4]Department of Life Science and Systems Engineering, Graduate School of Life Science and Systems Engineering, Kyushu Institute of Technology, Fukuoka 808-0196, Japan

Abstract

One of the most commonly used antibiotics for humans and animals is tetracycline (TC). TC can indirectly cause harmful impacts on the environment by enhancing the risk of antibiotic-resistant pathogens. Removing TC from water is challenging but crucial for human health. This work prepared TiO_2/PVDF film photocatalysts using the phase inversion method and evaluated their performance in degrading TC under UV light irradiation. The surface roughness and hydrophilicity of the TiO_2/PVDF film photocatalysts improved with increasing addition of TiO_2 to the photocatalyst films. The progress of TC degradation was monitored by UV–Vis spectroscopy, Liquid chromatography–mass spectroscopy (LC–MS), and chemical oxygen demand analysis. The PTi-6 film photocatalyst, comprised of 6 wt% TiO_2 and 12.5% PVDF, exhibited the highest TC degradation efficiencies. pH 5 is the optimum pH for tetracycline degradation using TiO_2/PVDF film. Based on the LC–MS results, the identified intermediates were used to propose the route of TC degradation. The PTi-6 film photocatalyst retained its photocatalytic efficiency for up to eight degradation cycles, proving the vast potential of the film to be applied in real-life situations.

Keywords Titanium dioxide, Polyvinylidene fluoride (PVDF), Photocatalysis, Tetracycline degradation

1 Introduction

The presence of pharmaceutical compounds in rivers, especially antibiotics, is a significant environmental and human health concern. The sources of antibiotics in rivers can be traced to the discharged effluent from manufacturing facilities, hospitals, veterinary clinics, livestock farms, and aquaculture industries [1]. In the aquaculture industry, only a small fraction of antibiotics is absorbed to prevent bacterial infections and parasitic diseases, with 80% of antibiotics being discharged and reaching various ecosystems [2]. Antibiotic consumption also increases tremendously with the rapid increase in the human population. After consumption, the antibiotic is partly metabolized in the biological system and eventually enters the aquatic environment through feces or urine. Of

more concerning note, the presence of these antibiotics in rivers enables the bacteria to develop resistance to them. According to a recently published study, antibiotic-resistant bacterial infections are the cause of the death of five million people in 2019 [3]. One of the various antibiotics contributing to this issue is tetracycline (TC).

TC is a broad-spectrum antibiotics used to treat microbial infections in human and animals [1]. Due to its extensive use and environmental persistence, its presence in the surface water, groundwater and drinking water has been detected [4], thereby prompting the use of numerous strategies, including microbial degradation, membrane filtration, ozonation, and adsorption to remove it from the water [5, 6]. However, these methods are less effective. Microbial degradation technique is unsuitable for removing antibiotics due to their antibacterial nature [6], membrane filtration suffers from membrane fouling [5] while adsorption efficiency of adsorbents is dependent on the pH of TC-containing solutions [7]. Although ozonation process can partially mineralize TC, it generally produces toxic byproducts [8]. Since finding an effective method of eliminating antibiotics is vital, it has attracted significant attention from researchers around the globe. Semiconductor photocatalysis, with TiO_2 as the most favoured photocatalyst, has been reported as a superior method in removing TC from water due to its efficiency, environmental friendliness and operates under mild condition [9]. The photocatalysts, upon activation by light absorption, generates highly reactive oxygen species such as hydroxyl and superoxide anion radicals which in turn can break down the TC molecules into benign end products. Even though there is much positive feedback on this technique, it has a major drawback that limits its large-scale applications. Since photocatalysts are conventionally used in powdered forms, several problems arise due to their inability to absorb UV light, due to aggregation of nanoparticles, uneven dispersion of particles in aqueous suspensions, and the time-consuming process of post-recovery of the nanoparticles from the treated wastewater [10].

Many researchers started immobilizing the photocatalyst onto a support to solve the post-recovery issue. Numerous inert substances have been used as support mediums, such as glass substrates [11], activated carbon [12], chitosan [13], and ceramics [14]. The use of polymeric membranes as support has also attracted significant interest. A recent review of the methods employed for immobilizing photocatalysts into and onto polymer membranes [15] and the application of these photocatalysts to degrade endocrine-disrupting chemicals has been published [16]. Choosing a suitable polymer that can work well with the photocatalysts is imperative to improve the separation process. The polymer should be stable under the photodegradation conditions and not be degraded by the photocatalyst.

In this work, we report TiO_2/PVDF photocatalyst film fabrication. PVDF was selected as a support material due to its high chemical and thermal resistance, mechanical strength, and high stability towards UV irradiation and vast oxidative conditions [17]. However, it has been reported that aged PVDF ultrafiltration membranes can produce microplastics when subjected to chemical cleaning processes [18]. Although there is a significant amount of literature on the fabrication of TiO_2/PVDF film, most studies focus on ultrafiltration, fouling studies, and degradation of dyes. The application of TiO_2/PVDF film in the photodegradation of pharmaceutical compounds, especially antibiotics, is minimal. This research focuses on determining the optimal formulation for preparing TiO_2/PVDF hybrid film photocatalyst and evaluating its potential to photodegrade TC

Table 1 The polymeric casting solution composition for TiO_2/PVDF film photocatalysts with different TiO_2 loading

PVDF wt%	TiO_2%	NMF wt %	Labelled as
Effect of TiO_2 content			
12.5	0	87.5	PTi-0
12.5	2	85.5	PTi-2
12.5	3	84.5	PTi-3
12.5	4	83.5	PTi-4
12.5	5	82.5	PTi-5
12.5	6	81.5	PTi-6
12.5	7	80.5	PTi-7

Table 2 The polymeric casting solution composition for TiO_2/PVDF film photocatalysts with different PVDF percentages

PVDF wt%	TiO_2 wt%	NMF wt %
Effect of percentages of PVDF		
7.5	6	86.5
10.0	6	84.0
15.0	6	79.0

under different reaction conditions. The reusability of the film is assessed to gauge the feasibility of using the TiO_2/PVDF in multicycle operations. The intermediates of tetracycline degradation, detected using liquid chromatography-mass spectrometry (LC-MS), are used to elucidate the degradation pathway.

2 Experimental

2.1 Materials

Polyvinylidene fluoride (PVDF, molecular weight = 534,000 g mol^{-1}), P25-TiO_2 powder, and pure N, N-dimethylformamide (NMF) solution were purchased from Sigma-Aldrich. Tetracycline (TC), 1,4-Benzoquinone (> 99%), Ethylenediaminetetraacetic acid (EDTA, > 99%), and tert-Butyl alcohol (99%) were purchased from Century, Acros Organic, R& M Chemical, and Riendemann Schmidt, respectively. Deionized water was used as the primary solvent in this work.

2.2 Formulation of TiO_2/PVDF membrane hybrid photocatalysts

The procedures for preparing nanoparticle/PVDF films using the phase inversion method [10]. In general, a certain amount of PVDF, according to the weight% ratio, was initially dissolved in N, N-dimethylformamide (NMF), followed by the addition of TiO_2 nanoparticles ranging from 0 to 7 wt% to produce the polymeric casting solution. While the amount of the PVDF, NMF, and TiO_2 used to prepare the TiO_2/PVDF film photocatalyst varies, as tabulated in Tables 1 and 2, the total weight of the casting solution was kept at 20 g. The casting solution was continuously stirred for 24 h for homogenous distribution of the nanoparticle photocatalyst material before the casting process was performed on a flat glass plate (8 cm× 10 cm) using a film casting knife to produce TiO_2/PVDF films with a thickness of 100 µm. The glass plate was then submerged in a coagulation bath containing deionized water for 24 h to completely separate the film from the glass plate and remove the impurities of the remaining solvents. Finally, the film was dried at room temperature for 24 h before it was further used in the photodegradation studies. Figure 1 illustrates the preparation of the hybrid film photocatalysts.

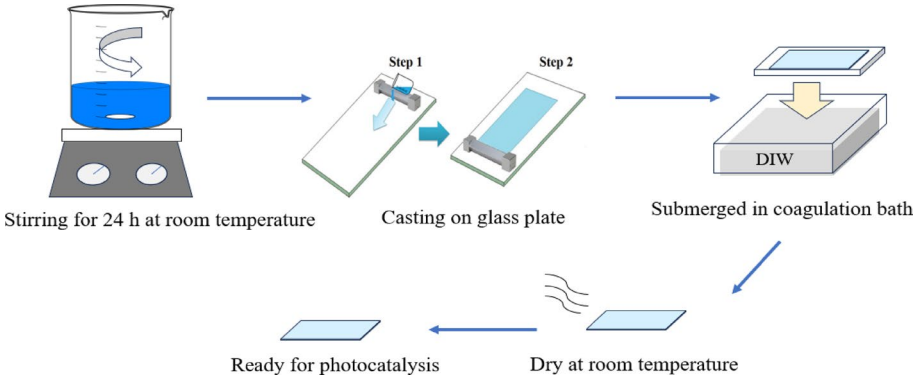

Fig. 1 Preparation of TiO_2/PVDF hybrid film photocatalyst

2.3 Characterization of the photocatalyst films

The TiO_2/PVDF film's physicochemical characteristics were investigated using several solid-state characterization techniques. X-ray diffractometer (PHILIPS PW 3040/60, Almelo, Netherlands) with CuKα radiation (30 kV, 30 mA) was used at a scanning range of $2\theta = 10°–80°$ to determine the phase and crystallinity of the films. Meanwhile, the film's surface morphology and elemental composition were recorded on a field emission-scanning electron microscope (FEI Nova NanoSEM 230) equipped with an electron-dispersive X-ray analyzer (HITACHI TM3000). An X-ray photoelectron spectrophotometer (Kratos Analytical Axis Ultra DLD) was used to identify the chemical state of the elements in the film. The film's surface roughness and wettability were estimated using an atomic force microscope (Seiko Instruments SPI 3800 N) and a water surface analysis system (VCA 3000 S).

2.4 Photodegradation of tetracycline

The photodegradation of TC was performed in a 1.0 L photoreactor (Fig S1). Two pieces of TiO_2/PVDF films were placed in the reactor, and 800 mL of 10 mg/L TC solution was added. For the first 30 min, the solution was stirred in the dark to allow the adsorption of TC on the photocatalyst film before being irradiated with a 7 W UVC lamp (254 nm, 15 mW/cm^2) for the next 5 h. Air was supplied using an aquarium pump throughout the degradation process. At preset time intervals, 5 mL of the solution was sampled and analysed using a UV-Vis spectrophotometer (PerkinElmer Lambda 35) at λ_{max} of 367 nm to determine the residual TC concentration. The flow chart of the TC photodegradation experiments is shown in Figure S2. The TC degradation percentage was calculated using Eq. 1, while the amount of TC degraded was determined using Eq. 2.

$$TC \text{ degradation } (\%) = \frac{C_0 - C_t}{C_0} \times 100 \tag{1}$$

$$\text{TC degraded } \left(\frac{\text{mg}}{\text{g}}\right) = \frac{C_0 - C_t \left(\frac{\text{mg}}{\text{L}}\right) \times \text{Volume of TC solution (L)}}{\text{weight of } TiO_2\text{/PVDF film (g)}} \tag{2}$$

C_0 and C_t are the TC concentrations at the initial and specific time intervals, respectively.

The performance of the films in degrading TC was also evaluated using chemical oxygen demand (COD) analysis. The COD of the TC solutions, measured using the closed reflux colorimetric method (APHA 5220 D), was estimated at different time intervals

by taking 2 ml of the TC solution and digesting it at 150 °C for 2 h in a fixed amount of oxidant reagent (Lovibond) using Thermo-reactor RD125 (Lovibond). A colorimeter (DR/890) was used to measure the COD and the COD percentages were calculated using Eq. 3.

$$\mathrm{COD}\ (\%) = \frac{\mathrm{COD_0} - \mathrm{COD_t}}{\mathrm{COD_0}} \times 100 \tag{3}$$

COD_0 and COD_t are the COD value at the initial and specific time (t) of the degradation, respectively.

The kinetics of TC degradation were investigated using the Langmuir-Hinshelwood (L–H) model. The rate of TC degradation, r, was calculated using Eq. 4, while the rate constant, $k_{obs,}$ can be determined from the slope of the ln C/C_0 vs. time plot (Eq. 5).

$$\mathrm{r} = -\mathrm{dC/dt} = \mathrm{k_{obs}C} \tag{4}$$

$$\ln \mathrm{C/C_0} = \mathrm{k_{obs}t} \tag{5}$$

2.5 Reusability test

To assess the stability and the reusability, the TiO_2/PVDF film photocatalyst was used in eight cycles of TC photodegradation experiments. were conducted on the pristine film to investigate their TC photodegradation capabilities under both UV light. At the end of each cycle, the film was thoroughly rinsed with deionized water to eliminate any surface contaminants. Subsequently, the film is returned into the photoreactor to begin degrading a fresh TC solution.

2.6 Liquid chromatography–mass spectroscopy (LC–MS) analysis

The identification of intermediates and photocatalytic degradation pathway for the degradation of TC was conducted using a Thermo Scientific C18 column (AcclaimTM Polar Advantage II) on an UltiMate 3000 UHPLC system (Dionex) equipped with a MicroTOF QIII Bruker Daltonic Mass analyzer. An eluent consisting of water, 0.1% Formic Acid, and 100% Acetonitrile was eluted at a gradient elution of 0.4 mL/min flow rate for 22 min at 40 °C column temperature. Positive ionization with 4500 V of capillary voltage was used during the LC-MS analysis.

3 Results and discussion

3.1 Characterization of TiO_2/PVDF films

The XRD pattern of powdered TiO_2 (Fig. 2a) shows the peaks characteristic of anatase TiO_2 at 2θ of 25.27° (101), 37.70° (004), 47.98° (200), 53.76° (105), 54.99° (211) and 62.57° (204) (JCPDS-21-1272), while a peak characteristic of rutile TiO_2 was observed at 2θ of 27.38° (110) (JCPDS-21-1276). Figure 2b shows the XRD pattern of pure PVDF and selected TiO_2/PVDF membrane film photocatalysts. The XRD pattern of the pure PVDF shows peaks characteristic of the PVDF α-phase at 2θ of 18.20° (020) and 19.08° (021) [19]. Upon the addition of TiO_2 into the PVDF film, characteristic peaks of anatase and rutile TiO_2 were observed. The intensity of these peaks increased as the TiO_2 weight percentages in the film increased, indicating the success of immobilising the TiO_2 nanoparticles.

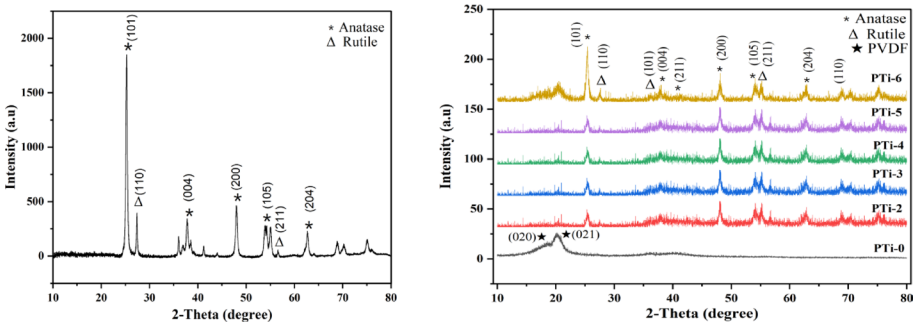

Fig. 2 XRD diffraction pattern of **a** TiO_2 nanoparticles and **b** TiO_2/PVDF films with TiO_2 loading from 0 to 6 wt %

The interaction, chemical characteristics, and elemental composition of TiO_2/PVDF film photocatalysts were investigated using X-ray photoelectron spectroscopy (XPS). The XPS survey spectrum shows peaks of the main components of the TiO_2/PVDF film photocatalyst: Ti, F, C, and O (Fig. 3a). Three peaks (Fig. 3b) were observed at 284.85 eV, 285.3 eV, and 289.35 eV for the C 1s peak, which can be correlated to the C–C bond, C–F sp^3, and C-H bond, respectively that corresponds to the PVDF molecular structure [20]. The peaks at 529.35 eV, 531.0 eV, and 533.05 eV binding energy for the O 1s spectrum (Fig. 3c) were attributed to the formation of Ti–O–Ti, Ti–OH, and the hydrogen bonding between the O of TiO_2 and H of adsorbed water on the PVDF film, respectively [21]. The possibility of hydroxyl groups (–OH) at the surface of TiO_2 nanoparticles that enhance the water-dispersibility of TiO_2 for effective photocatalytic performance was reported in previous literature [22]. The F1s spectrum (Fig. 3d) shows the peak observed at a binding energy of 684.75 eV, attributed to the C–F semi-ionic bond [20]. The binding energy for Ti 2p shows peaks at 458.55 eV and 464.86 eV (Fig. 3e), which are attributed to Ti $2p^{3/2}$ and Ti $2p^{1/2}$, respectively. The binding energy difference of 5.0 eV indicates the presence of Ti^{4+} in the TiO_2/PVDF film [23].

Figure 4 shows the surface morphology of the pristine PVDF and TiO_2/PVDF films (FESEM images) and their respective EDX analysis. Pristine PVDF and TiO_2/PVDF film photocatalysts showed a porous surface on the photocatalyst film. For the TiO_2/PVDF photocatalyst films, a good distribution of TiO_2 particles was observed on the PVDF surface. Among all the TiO_2/PVDF film photocatalysts, PTi-6 showed the most extensive distribution of TiO_2 on the photocatalyst film. TiO_2 loading higher than 6 wt% (PTi-7) resulted in the blockages of the porous site areas of the PVDF with fewer TiO_2 nanoparticles on the film surface. This occurrence might be attributed to the highly viscous casting solution at high TiO_2 content, which leads to poor segregation and uneven distribution of TiO_2 nanoparticles in the casting solution. The poor absorption of light and pollutant-catalyst absorption will eventually decrease the degradation performance of the film photocatalyst in degrading tetracycline antibiotics [24].

The EDX spectra of the TiO_2/PVDF film photocatalysts also show increasing TiO_2 content with growing amounts of TiO_2 particles added to the casting solution while preparing the TiO_2/PVDF.

film photocatalysts. This confirms the successful immobilisation of TiO_2 nanoparticles into the PVDF film. A film photocatalyst's surface roughness and hydrophilicity are essential to achieve the best photocatalytic performance. A rough surface leads to high hydrophilicity, better wettability, and more significant interaction between the

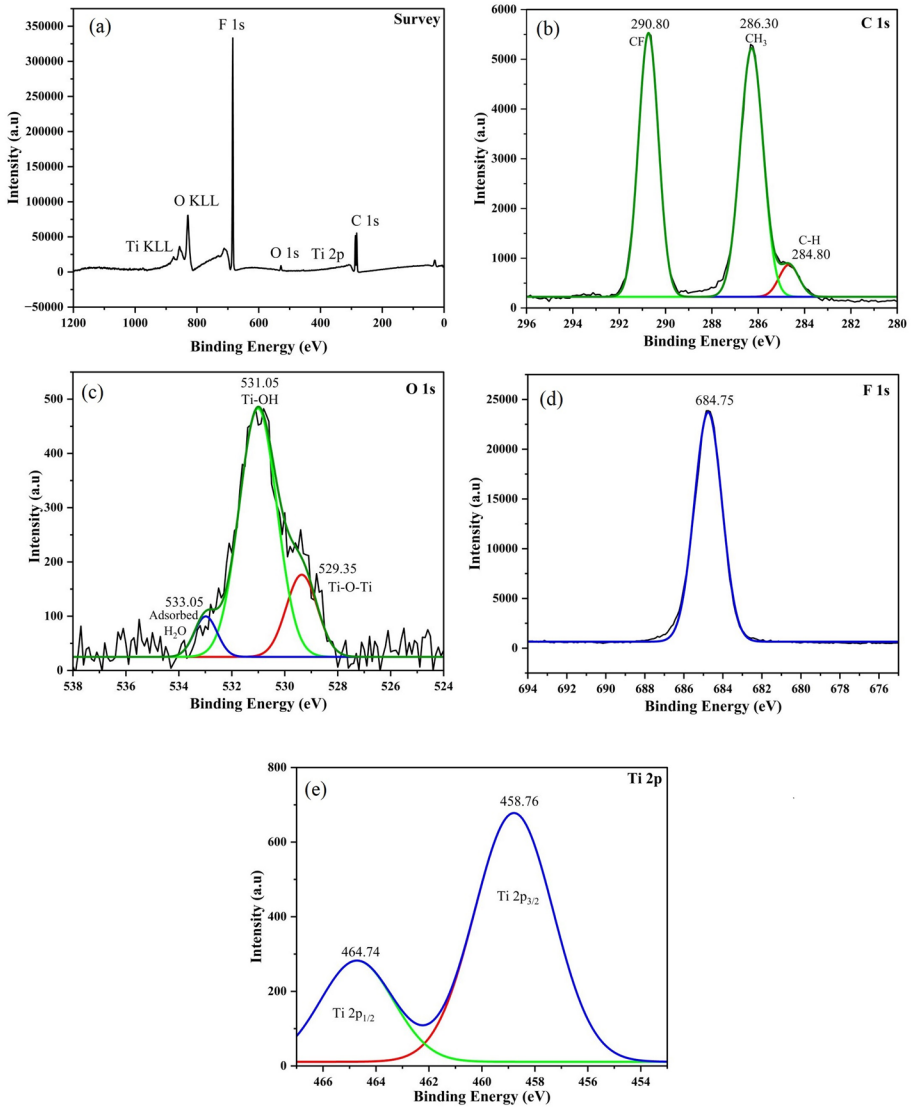

Fig. 3 XPS spectra of the **a** survey, **b** C 1s, **c** O 1s, **d** F 1s, and **e** Ti 2p in the PTi-6 film photocatalyst

pollutants and the surface of the photocatalyst film [25]. The surface roughness and the hydrophilicity of the neat PVDF and TiO_2/PVDF hybrid films, observed via atomic force micrographs and water contact angles, are shown in Fig. 5.

As depicted by the 2-D and 3-D micrographs, the roughness of the surface increased from 0.0038 μm to 0.0415 μm with the increasing amount of TiO_2 immobilised on the PVDF film, which is similar to a previously reported study [26]. However, the water contact angle of the films decreased with increasing TiO_2 content, indicating an increase in the hydrophilic properties of the film. This phenomenon can be attributed to increasing surface hydroxyl groups (Ti-OH) as more TiO_2 particles are embedded in the PVDF film. In addition to the C-F group in the PVDF structure, these groups can form hydrogen bonds with water molecules, consequently increasing the hydrophilicity of the TiO_2/PVDF film.

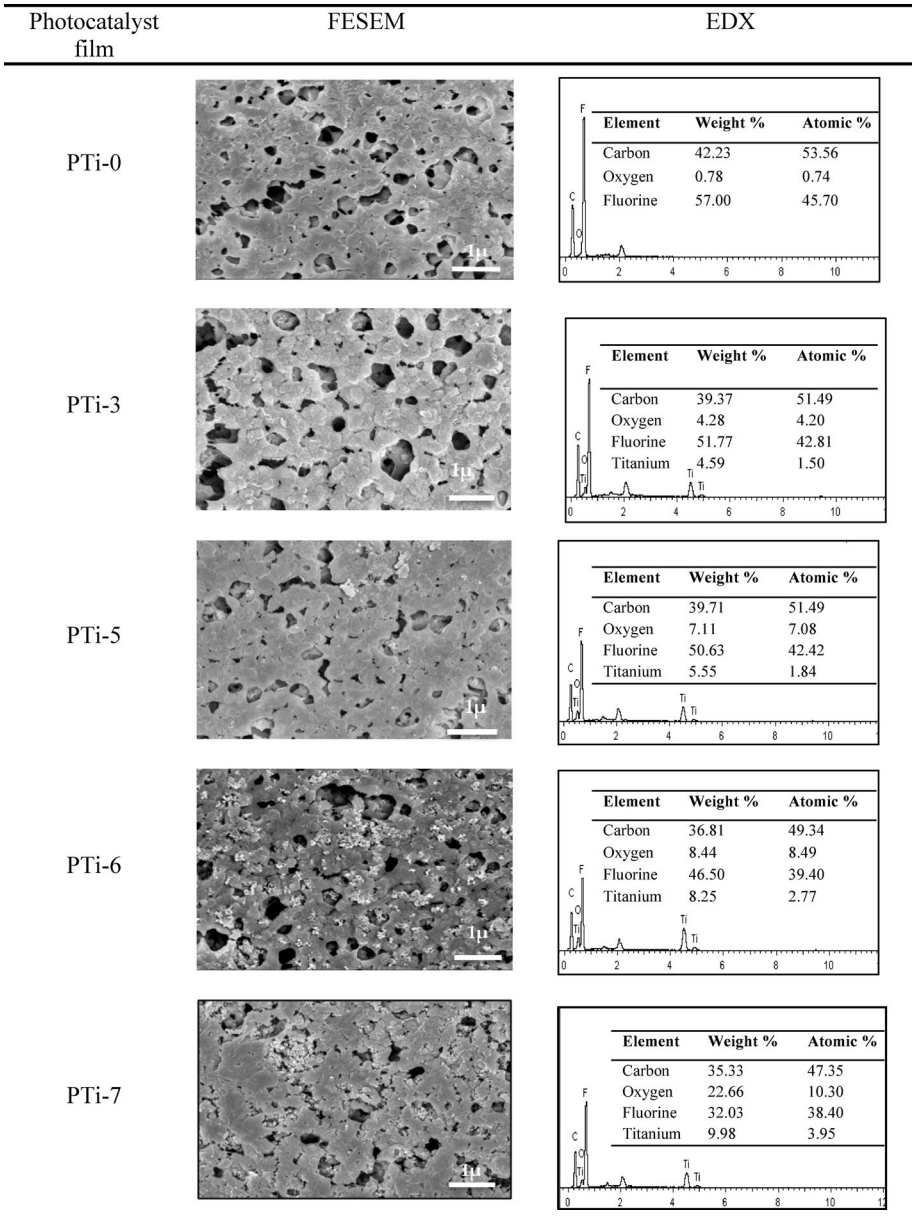

Fig. 4 FESEM-EDX analysis of TiO_2/PVDF film photocatalysts

3.2 The photocatalytic activity of TiO_2/PVDF films

3.2.1 Screening of the photocatalyst film

The performance of the TiO_2/PVDF films in degrading tetracycline (TC) solution was investigated under five hours of UV light irradiation. Prior analysis shows that the TC is stable towards UV irradiation. The adsorption of TC on the film is less than 10%. Figure 6; Table 3 show the comparative photocatalytic performance of the prepared photocatalyst films. PTi-6 exhibits the highest photocatalytic performance, indicating that 6 wt% of TiO_2 is the optimum amount of TiO_2 that can be immobilized into the PVDF film without sacrificing its photocatalytic performance (Fig. 6a). The capability of PTi-6 to photodegrade 94% of TC at the rate of 0.102 mg/L min could be attributed to its physicochemical characteristics, i.e., well-dispersed TiO_2 particles on the surface and high surface roughness and hydrophilicity. A slightly lowered photocatalytic performance

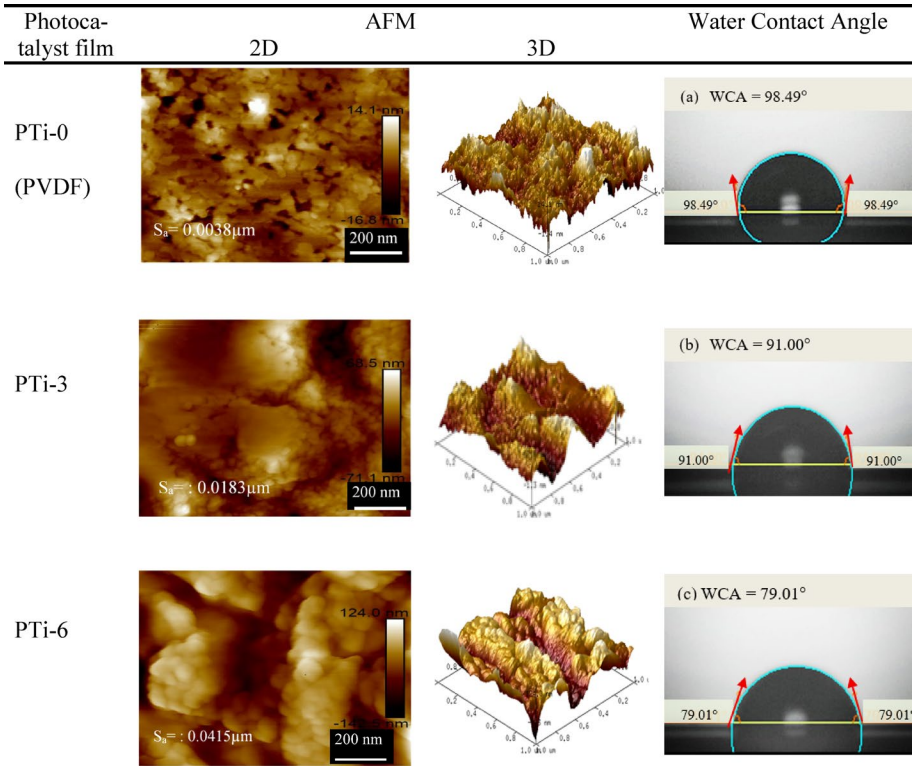

Fig. 5 Surface images of 2-D and 3-D and the water contact angle for PVDF and TiO_2/PVDF film

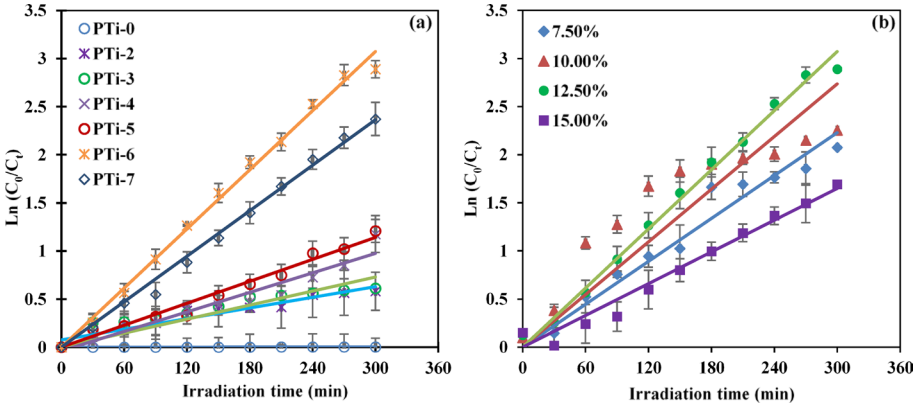

Fig. 6 Screening for the best film photocatalyst; photocatalytic degradation efficiencies of TiO_2/PVDF with various loading of **a** TiO_2 and **b** PVDF. (TC volume: 0.8 L, number of films photocatalyst used: 2 films, $[TC]_0$: 10 mg/L, pH of TC: 5.8)

observed for PTi-7 could be due to particle agglomeration, which decreased the available sites for photocatalytic degradation and inefficient light absorption.

The effect of PVDF content on photocatalytic efficiency is reflected in Fig. 6b. The photocatalytic efficiency of the film increases with increasing percentage of PVDF in the casting solution to an optimum amount of 12.5 wt% before it decreases at 15 wt% %. At 15 wt%, the viscosity of the casting solution was the highest, which led to poor dispersion of the TiO_2 on the surface of the photocatalyst film and consequently reduced the photocatalytic performance of the film. Based on these results, the best photocatalyst

Table 3 The effect of different catalyst loading (0–7%) using TiO_2/PVDF photocatalyst film on kinetic data and the amount of TC degraded

Sample	Degradation efficiency (%)	k_{obs} (min^{-1})	Rate (mg/L min)	Amount of TC degraded (mg/g)	Correlation factor (R^2)
PTi-0	0.37	1.0×10^{-5}	1.0×10^{-4}	3.4	0.8307
PTi-2	44.12	0.0018	0.019	9.1	0.9422
PTi-3	45.79	0.0018	0.018	10.0	0.9037
PTi-4	69.15	0.0034	0.034	11.1	0.9343
PTi-5	70.15	0.0039	0.039	11.2	0.9777
PTi-6	94.44	0.0102	0.102	12.9	0.9943
PTi-7	90.67	0.0082	0.082	11.0	0.9958
Percentages of PVDF (%)	**Degradation efficiency (%)**	**k_{obs} (min^{-1})**	**Rate (mg/L min)**	**Amount of TC degraded (mg/g)**	**Correlation factor (R^2)**
7.5	84.56	0.0077	0.0770	10.4	0.9944
10	89.43	0.0082	0.0820	10.9	0.9817
12.5	94.44	0.0102	0.1020	12.9	0.9943
15	81.62	0.0060	0.0060	10.0	0.9871

film formulation contained 6 wt% TiO_2 and 12.5 wt% PVDF. Hence, PTi-6 was considered the best TiO_2/PVDF film photocatalyst.

3.2.2 Effect of reaction conditions

The performance of PTi-6 to photodegrade TC was further investigated under different reaction conditions. Figure 7a illustrates the effect of TC concentration on the degradation efficiency. The percentage of TC degradation decreases with increasing TC concentration. As the concentration of TC increases, the ratio of TC molecules to the active photocatalytic sites increases, explaining the reduction in the percentage degradation of TC. Moreover, the presence of intermediates competing for the surface catalyst's active site also contributes to the observed decrement [27]. The effect of catalyst loading on the degradation efficiency was investigated using different numbers of the PTi-6 film. A maximum of 4 pieces of the film were used due to the photoreactor configuration. The efficiency of TC degradation increases with the number of films used (Fig. 7b). A complete TC degradation with the fastest rate of 0.24 mg/L min was observed when 4 pieces of the PTi-6 film were used. The results also reflect the advantage of using film over powdered photocatalyst, as the degradation efficiency of the latter process is affected by the agglomeration of the catalyst and the increasing turbidity of the solution at higher loading of powdered photocatalyst [28].

The changes in the pH of the TC solution will affect not only the TC's speciation but also the film photocatalyst's surface charge. The TC molecule has three pK_a values (3.3, 7.7, and 9.7) and can exist as cationic, zwitterion, and anionic species in acidic, mildly acidic-neutral, and basic conditions, respectively. The pH of zero-point charge (pH_{zpc}) of TiO_2 was 6.2, indicating that the film is positively charged at pH below 6.2 and negatively charged at pH above 6.2 [29]. Figure 7c illustrates the effect of the TC solution's pH on the degradation efficiency. The TC degradation percentage increases when the pH increases to pH 5 and then gradually decreases at higher pH values. The highest percentage of TC degradation at pH 5 is attributed to a stronger interaction the reaction was

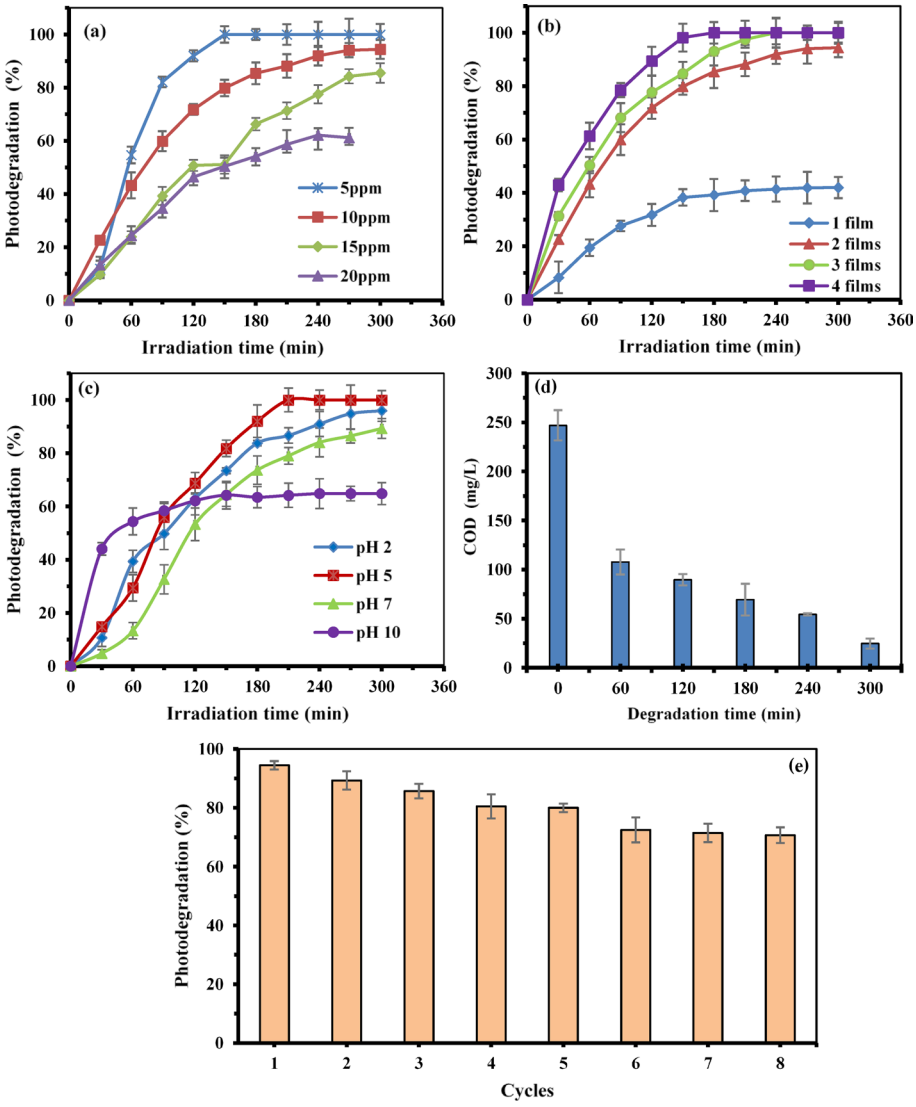

Fig. 7 The photodegradation TC at different **a** TC concentration, **b** number of film and **c** pH; **d** the COD analysis the reusability of the film and **e** recyclability study (Conditions: number of films photocatalyst used: 2 films, $[TC]_0$: 10 mg/L, pH = 5.8, unless stated otherwise)

unaffected, proving that the films are stable in acidic and basic media. The between the TC, which has an anionic moiety, and the positively charged film. The TC and the film's surface became negatively charged at higher pH values, resulting in a decreased TC degradation efficiency due to the repulsion effect [30]. The weight of the photocatalyst film afterprogress of the TC degradation is also monitored using chemical oxygen demand (COD) analysis. Figure 7d shows that the total oxygen required to oxidize TC decreases from 247 mg/L to 24.67 mg/L with time, indicating the degradation of the TC by the PTi-6 film photocatalyst. Subsequently, the complete mineralization of TC required more than 5 h of irradiation. The gradual decrease could be attributed to the accumulation of undegraded compounds, as reflected by the COD analysis, on the surface of the photocatalyst film.

3.2.3 Reusability test

The capability of the PTi-6 hybrid film photocatalyst to be used in a multicycle of the TC degradation process is depicted in Fig. 7e. The photodegradation efficiency decreases gradually up to the eighth cycle from 94% (fresh film) to 71%. It was found that the film can maintain its good performance after being repeatedly applied for the degradation of TC. The decrease in the photocatalytic activity using recycled photocatalyst might be attributed to some TiO_2 particles peeling off from the film's surface into the sample solution due to the vigorous stirring of the sample solution for long hours. The reusability study was discontinued due to the structural integrity problem, as the film was torn at the end of the eighth cycle.

3.3 Photodegradation mechanism and TC degradation pathways

To envisage the TC degradation mechanism, 10 mL of 0.1 mol/L radical-scavenging solutions namely,1,4-benzoquinone (*p*-BQ), ethylenediaminetetraacetic acid (EDTA), and *tert*-butanol (*t*-BuOH), were added separately into the TC solution to react with the $\cdot O_2^-$, h^+ and ·OH radicals, respectively. As illustrated in Fig. 8a, the photocatalytic degradation of TC was severely affected by the presence of *p*-BQ, with a reduction efficiency of 81% indicating that the $\cdot O_2^-$ is the main species responsible for the effective degradation of TC. Thus, the proposed TC degradation mechanism on the photocatalyst's surface is illustrated in Fig. 8b.

When the photocatalyst surface absorbed the light, a photoexcitation process was initiated where the negatively charged electrons (e^-) from the valence band (VB) jumped to the higher energy band, which is the conduction band (CB), leaving a positive charge hole (h^+) on the valence band. The photogenerated holes at the valence band can oxidize the adsorbed water to produce a very reactive hydroxyl radical, ·OH. Meanwhile, the photogenerated electron at the conduction band can reduce the adsorbed oxygen on the catalyst's surface, forming superoxide radical anions, $\cdot O_2^-$ (Eq. 6). The superoxide radical anions can also react with the H^+ ion that exists in the solution to form hydroperoxyl radical species (·OOH), hydroperoxyl anion, HOO^-, and further form hydrogen peroxide, H_2O_2 (Eqs. 7–10). These generated species can directly attack the pollutant or react with oxygen or water molecules to produce potent oxidizing hydroxyl radicals, which promote the oxidation of TC antibiotics (Eqs. 11–13) [31].

$$O_2 + e_{cb}^- \rightarrow \cdot O_2^- \tag{6}$$

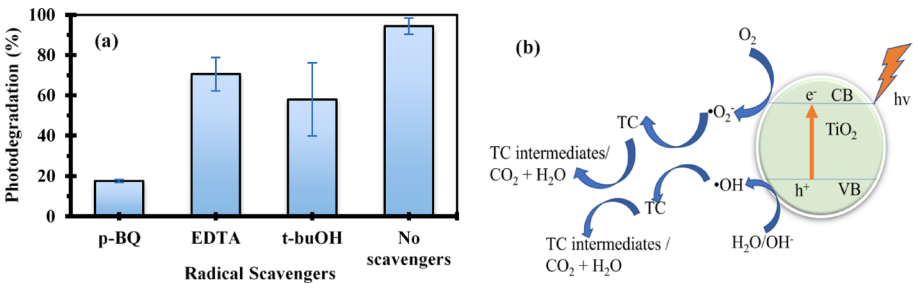

Fig. 8 **a** Percentages of degradation percentage of TC with the presence of three type of radical scavengers using PTi-6 film photocatalyst for five hours under UV light (Conditions: $[TC]_0$ = 10 mg/L; [Radical Scavenger] used = 0.1 mol/L; Number of films = 2; pH = 5.8) and **b** The possible mechanism of photodegradation of TC on the surface of TiO_2/PVDF film photocatalyst

$$\cdot O_2^- + h^+ \rightarrow \cdot OOH \tag{7}$$

$$\cdot OOH + e_{cb}^- \rightarrow HOO^- \tag{8}$$

$$HOO^- + H^+ \rightarrow H_2O_2 \tag{9}$$

$$H_2O_2 + e_{cb}^- \rightarrow OH^- + \cdot OH \tag{10}$$

$$\cdot OH + TC \rightarrow \text{mineralization of TC} \tag{11}$$

$$\cdot O_2^- + TC \rightarrow \text{mineralization of TC} \tag{12}$$

$$\cdot OOH + TC \rightarrow \text{mineralization of TC} \tag{13}$$

The photocatalytic degradation of tetracycline (TC) by PTi-6 was further investigated using LC–MS/MS to detect the intermediates and fragments formed. The characteristic peak of TC ($m/z = 445$) was observed at a retention time of 7.6 min. Table 4 shows the gradual decrease in the characteristic peak intensity, indicating the progressive degradation of the TC, and the mass-charge ratio (m/z) data of the TC fragments obtained from the LC–MS/MS spectra, with increasing reaction time. The chemical structure of the TC fragments was constructed according to their m/z ratio.

After 30 min of reaction time, peaks at m/z = 401, 428, and 431 were observed, indicating three initial possible degradation pathways for the destruction of the tetracycline compound through the elimination of the C=O(NH_2) group, NH_2, and the CH_3 group, respectively. According to Xie et al. [32], the NH_2 and CH_3 functional groups can be an easy target for the initial attack of radical species. The molecules were further degraded via elimination of (CH)=C(OH), OH, and (C_6H_4)OH group to produce fragments with m/z values of 369, 411, and 366, respectively, after 1 h of reaction. As the reaction proceeded, more degradation products with smaller and simpler molecular structures were identified. Fragments with m/z values of 354, 301, 287, 282, 252, 227, and 205 indicate more bond breaking, and ring crackings within the structure of TC were detected after 3 h of reaction time, respectively. After 5 h of irradiation time, almost all of the rings in the molecular structure have been cracked, producing smaller fragments with an m/z ratio of less than 200. The compounds can be further degraded to less hazardous final products, such as CO_2, H_2O, and NH_4^+. Based on these analyses, the possible degradation pathway of tetracycline is illustrated in Fig. 9. Some of these fragments have been reported in previous literature works [33, 34].

Table 4 LC–MS/MS data for tetracycline compound and its intermediates

Degradation time (h)	Intensity of tetracycline (m/z 445.16)	Retention time (min)	List of main intermediates with m/z
30 min	209,004	7.6	401.17, 428.00, 430.91
1	84,858	7.6	369.10, 411.12, 366.13
2	40,339	7.6	301.14, 354.06, 252.00, 282.15
3	10,993	7.6	205.07, 205.11, 227.16, 287.12, 252.00, 287.12
4	10,437	7.6	187.08, 195.12, 205.07, 224.02,126.00, 168.08
5	6648	7.6	121.03, 114.10, 110.03, 124.99, 101.00

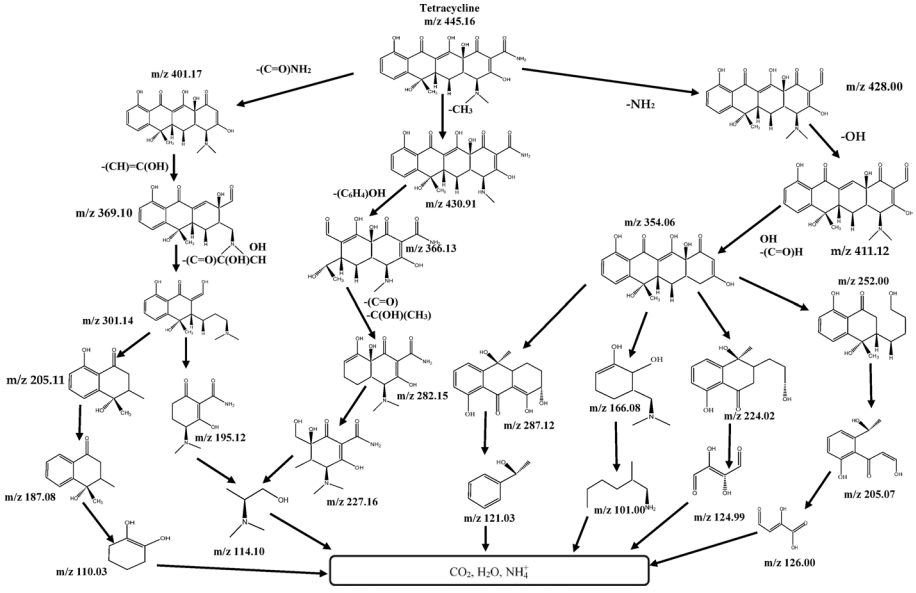

Fig. 9 The possible photocatalytic degradation pathway of tetracycline for 5 h of UV irradiation

4 Conclusions

This study successfully developed an effective TiO_2/PVDF film photocatalyst, PTi-6, comprising 6 wt% TiO_2 and 12.5 wt% PVDF for TC degradation. The high efficiency of the PTi-6 film photocatalyst is due to its high porosity, surface roughness, and hydrophilicity, which enable a good interaction between the TC and the surface of the photocatalyst. Two pieces of the PTi-6 could photodegrade 94% of 10 mg/L TC within five hours of UV irradiation at pH 5. A complete TC degradation at a much faster rate can be achieved with the increasing number of films used. LCMS detected various intermediate products during the degradation of TC under UV light, and the possible degradation pathways were successfully proposed according to the fragments found from the LC-MS data. The PTi-6 film photocatalyst exhibited a slight decrease in degradation efficiencies up to the eighth cycle, which proved the stability of the film photocatalyst and its potential to be applied for actual wastewater treatment.

Supplementary Information

The online version contains supplementary material available at https://doi.org/10.1186/s11671-025-04384-7.

Supplementary Material 1

Acknowledgements

The authors gratefully acknowledged the financial support from Universiti Putra Malaysia and Kyushu Institute of Technology for the UPM-Kyutech Collaborative Grant (UPM.RMC/800/2/2/4/Matching UPM-KYUTECH/2021/ 9300479), Universiti Teknologi Mara for the scholarship awarded to Hazlini Mohmad Ameran, and Universiti Putra Malaysia and Universiti Kebangsaan Malaysia (XPS and LCMS) for the technical and management support to conduct the research work.

Author contributions

Conceptualization - AHA, YPT, TO and YA; Methodology - AHA, YPT, TO and YA; Data collection - HMA; formal analysis - HMA, ENM, AHA, TO; writing—original draft preparation- HMA.; writing—review and editing - AHA, TYP, TO; supervision- AHA YPT and ENM. All authors have read and agreed to the published version of the manuscript.

Funding

This study was funded by Universiti Putra Malaysia-Kyutech Collaborative Grant (UPM.RMC/800/2/2/4/Matching UPM-KYUTECH/2021/9300479). Hazlini Mohmad Ameran received a scholarship for her PhD candidacy from Universiti Teknologi Mara, Malaysia.

Data availability
Data are available upon request.

Declarations

Ethics approval
Not applicable.

Consent to participate
Not applicable.

Consent to publish
Not applicable.

Competing interests
The authors declare no competing interests.

Received: 21 July 2025 / Accepted: 3 November 2025
Published online: 15 November 2025

References

1. Liu C, Tan L, Zhang L, Tian W, Ma L. A review of distribution of antibiotics in water in different region of China and current antibiotic degradation pathway. Front Environ Sci. 2021;9:692298. https://doi.org/10.3389/fenvs.2021.692298.
2. Tiwari A, Shukla A, Lalliansanga TD, Lee S-M. Au-nanoparticle/Nanopillars TiO_2 meso-porous, thin films in the degradation of tetracycline using UV-A light. J Ind Eng Chem. 2020;69:141–52. https://doi.org/10.1016/j.jcis.2020.12.014.
3. Murray CJL, Ikuta KS, Sharara F, et al. Global burden of bacterial antimicrobial resistance in 2019. A systematic analysis. Lancet. 2022;399(10325):629–55.
4. Xu L, Zhang H, Xiong P, Zhu Q, Liao C, Jiang G. Occurrence, fate, and risk assessment of typical tetracycline antibiotics in the aquatic environment: a review. Sci Total Environ. 2021;753:141975.
5. Gopal G, Alex SA, Chandrasekaran N, Mukherjee A. A review on tetracycline removal from aqueous systems by advanced treatment techniques. RSC Adv. 2020;10(45):27081–95. https://doi.org/10.1039/d0ra04264a.
6. Lu Z-Y, Zhang J-T, Fan N-S, Huang B-C, Jin R-C. A critical review of antibiotic removal strategies: performance and mechanisms. J Water Process Eng. 2020;38:101681. https://doi.org/10.1016/j.jwpe.2020.101681.
7. Althumayri K, Guesmi A, El-Fattah WA, Houas A, Hamadi NB, Shahat A. Enhanced adsorption and evaluation of tetracycline removal in an aquatic system by modified silica nanotubes. ACS Omega. 2023;8(7):6762–77. https://doi.org/10.1021/acsomega.2c07377.
8. Żyłła R, Ledakowicz S, Boruta T, Olak-Kucharczyk M, Foszpańczyk M, Mrozińska Z, Balcerzak J. Removal of tetracycline oxidation products in the nanofiltration process. Water. 2021;13(4):555. https://doi.org/10.3390/w13040555.
9. Ma J, Chen Y, Zhou G, Ge H, Liu H. Recent advances in photocatalytic degradation of tetracycline antibiotics. Catalysts. 2024;14:762. https://doi.org/10.3390/catal14110762.
10. Mohd Hir ZA, Abdullah AH, Zainal Z, Lim HN. Visible light-active hybrid film photocatalyst of polyethersulfone–reduced TiO_2: photocatalytic response and radical trapping investigation. J Mater Sci. 2018;53(18):13264–79. https://doi.org/10.1007/s10853-018-2570-3.
11. Tian S, Feng Y, Zheng Z, He Z. TiO_2-based photocatalytic coatings on glass substrates for environmental applications. Coatings. 2023;13:1472. https://doi.org/10.3390/coatings13081472
12. Rajendran S, Inwati GK, Yadav VK, Choudhary N, Solanki MB, Abdellattif MH, Yadav KK, Gupta N, Islam S, Jeon BH. Enriched catalytic activity of TiO_2 nanoparticles supported by activated carbon for noxious pollutant elimination. Nanomaterials. 2021;11:2808. https://doi.org/10.3390/nano11112808.
13. Anaya-Esparza LM, Ruvalcaba-Gómez JM, Maytorena-Verdugo CI, González-Silva N, Romero-Toledo R, Aguilera-Aguirre S, Pérez-Larios A, Montalvo-González E. Chitosan-TiO_2: a versatile hybrid composite. Materials. 2020;13(4):811. https://doi.org/10.3390/ma13040811.
14. Danfá S, Martins RC, Quina MJ, Gomes J. Supported TiO_2 in ceramic materials for the photocatalytic degradation of contaminants of emerging concern in liquid effluents: a review. Molecules. 2021;26(17):5363. https://doi.org/10.3390/molecules26175363.
15. Zakria HS, Othman MHD, Kamaludin RSH, Kadir SA, Kurniawan TA, Jilani A. Immobilization techniques of a photocatalyst into and onto a polymer membrane for photocatalytic activity. RSC Adv. 2021;11(12):6955–7014. https://doi.org/10.1039/d0ra10964a.
16. Mohd Hir ZA, Abdullah AH. Hybrid polymer-based photocatalytic materials for the removal of selected endocrine disrupting chemicals (EDCs) from aqueous media: a review. J Mol Liq. 2022;361:119632. https://doi.org/10.1016/j.molliq.2022.119632.
17. Zou D, Lee YM. Design strategy of poly(vinylidene fluoride) membranes for water treatment. Prog Polym Sci. 2022;128:101535. https://doi.org/10.1016/j.progpolymsci.2022.101535.
18. Gan X, Lin T, Jiang F, Zhang X. Impacts on characteristics and effluent safety of PVDF ultrafiltration membranes aged by different chemical cleaning types. J Membr Sci. 2021;640:119770. https://doi.org/10.1016/j.memsci.2021.119770.
19. Zhao X, Lana Y, Yang K, Wang R, Cheng L, Gao C. Antifouling modification of PVDF membranes via in situ mixed-charge copolymerization and TiO_2 mineralization. Appl Surf Sci. 2020;525:146564. https://doi.org/10.1016/j.apsusc.2020.146564.
20. Zhang L, Shi X, Zhao M, Yin Z, Zhang J, Wang S, Du W, Xiang J, Cheng P, Tang N. Construction of precisely controllable and stable interface bonding Au-TiO_2/PVDF composited membrane for biofouling-resistant properties. Surf Interfaces. 2021;24:101152. https://doi.org/10.1016/j.surfin.2021.101152.

21. Wu Z, Liang Y, Yuan X. MXene Ti_3C_2 derived Z–scheme photocatalyst of graphene layers anchored TiO_2/g–C_3N_4 for visible light photocatalytic degradation of refractory organic pollutants. Chem Eng J. 2020;394:124921. https://doi.org/10.1016/j.cej.2020.124921. ´Zou D, Fang J, Jiang L, Zhang J, Yang H, Xiao Z.
22. Kipreos MD, Foster M. Water interactions on the surface of 50 Nm rutile TiO_2 nanoparticles using in situ DRIFTS. Surf Sci. 2018;677:1–7. https://doi.org/10.1016/j.susc.2018.05.005.
23. Zheng X, Liu Y, Liu X, Li Q, Zheng Y. A novel PVDF-TiO_2@g-C_3N_4 composite electrospun fiber for efficient photocatalytic degradation of tetracycline under visible light irradiation. Ecotox Environ Safe. 2021;210:111866. https://doi.org/10.1016/j.ecoenv.2020.111866.
24. Chanu LA, Singha WJ, Singh KJ, Devia KN. Effect of operational parameters on the photocatalytic degradation of methylene blue dye solution using manganese doped ZnO nanoparticles. Results Phys. 2019;12:1230–7. https://doi.org/10.1016/j.rinp.2018.12.089.
25. Wang Y, Li Q, Miao W, Lu P, You C, Wang Z. Hydrophilic PVDF membrane with versatile surface functions fabricated via cellulose molecular coating. J Membr Sci. 2021;640:119817. https://doi.org/10.1016/j.memsci.2021.119817.
26. Rafiei H, Abbasian M, Yegani R. Polyvinylidene fluoride as a neat and the synthesized novel membranes based on PVDF/polyvinyl pyrrolidone polymer grafted with TiO_2 nanoparticles through RAFT method for water purification. Iran Polym J. 2021;30(8):769–80. https://doi.org/10.1007/s40820-023-01146-x.
27. Qu J, Cao X, Gao L, Li J, Lu L, Xie Y, Zhao Y, Zhang J, Wu M, Liu H. Electrochemical carbon dioxide reduction to ethylene: from mechanistic understanding to catalyst surface engineering. Nano-Micro Lett. 2023;15(1):178. https://doi.org/10.1007/s40820-023-01146-x.
28. Seyyedbaghari H, Alizadeh R, Mirzayi B. Visible light driven impressive activation of persulfate by Bi_5O_7Br-modified ZnO for photodegradation of tetracycline: facile synthesis, kinetic and mechanism study. J Mol Liq. 2022;365:120176. https://doi.org/10.1016/j.molliq.2022.120176.
29. Rajagopal S, Paramasivam B, Muniyasamy K. Photocatalytic removal of cationic and anionic dyes in the textile wastewater by H_2O_2 assisted TiO_2 and micro-cellulose composites. Sep Purif Technol. 2020;252:117444. https://doi.org/10.1016/j.seppur.2020.117444.
30. Afzal MZ, Zu P, Zhang CM, Guan I, Song C, Sun XF, Wang SG. Sonocatalytic degradation of Ciprofloxacin using hydrogel beads of TiO_2 incorporated biochar and chitosan. J Hazard Mater. 2022;434:128879. https://doi.org/10.1016/j.jhazmat.2022.128879.
31. Zhou H, Wang H, Yue H, He L, Li H, Zhang H, Yang S, Ma T. Photocatalytic degradation by TiO_2-conjugated/coordination polymer heterojunction: preparation, mechanisms, and prospects. Appl Catal B. 2024;344:123605. https://doi.org/10.1016/j.apcatb.2023.123605.
32. Xie ZH, He CS, Zhou HY, Li LL, Liu Y, Du Y, Liu W, Mu Y, La B. Effects of molecular structure on organic contaminants' degradation efficiency and dominant ROS in the advanced oxidation process with multiple ROS. Environ Sci Technol. 2022;56(12):8784–95. https://doi.org/10.1021/acs.est.2c00464.
33. Kubiak A, Bielan Z, Kubacka M, Gabała E, Grześkowiak AZ, Janczarek M, Zalas M, Anna, Jurek AZ, Ciesielczyk KS, Jesionowski T. Microwave-assisted synthesis of a TiO_2-CuO heterojunction with enhanced photocatalytic activity against tetracycline. Appl Surf Sci. 2020;520:146344. https://doi.org/10.1016/j.apsusc.2020.146344.
34. Serra A, Gomez E, Michler J, Philippe L. Facile cost-effective fabrication of Cu@Cu_2O@CuO–microalgae photocatalyst with enhanced visible light degradation of tetracycline. Chem Eng J. 2021;413:127477. https://doi.org/10.1016/j.cej.2020.127477.

Publisher's note